Journal of Medical Imaging and Health Informatics
Vol. 7, 897–902, 2017

Radiotherapy Treatment Based on Binocular Location: Real-Time Monitoring System of Patient Setup Errors

Lei Chai[1], Da Chen[1], Xiao-Bin Tang [1,*], Yun Ge[2], Ying Chen[2], Jun Li[1], and Quan-Bo Wei[2]

[1]*Department of Nuclear Science and Engineering, Nanjing University of Aeronautics and Astronautics, 210016, China*
[2]*School of Electronic Science and Engineering, Nanjing University, 210046, China*

Purpose: We aim to develop a new method in order to achieve the real-time monitoring of the patient movement (translation and rotation), and to evaluate the accuracy of our proposed method. *Methods and Materials*: Orientation Registration Apparatus (ORA) have been developed to register the initial orientation of the Computed Tomography (CT) coordinate system. Based on binocular location, the translations in left to right (LR), inferior to superior (IS), anterior to posterior (AP) directions and rotations in roll, pitch, and yaw directions can be measured in real-time. We conducted 50 experiments under different conditions in order to verify the accuracy of this method, we divided these 50 experiments into five sets. In each set, the number of markers affixed to phantom was the same, but the relative position between markers and treatment center were different. Between set and set, there were different numbers of markers affixed to phantom. In each experiment, we compared the absolute position and relative movement between the actual value and the measured value by our method. *Results*: In our experiments, the precision of the absolute location in the LR, IS, and AP directions is 0.5 mm, and that in the roll, pitch and yaw directions is 0.5°. For the relative location, the precision is the same inside the monitoring scope; and for the stable precision, there should be 6 markers affixed to the phantom that is a representation of a patient. *Conclusion*: This study indicates that our method has an accuracy of 0.5 mm in translations and 0.5° in rotations, and can monitor the position and rotation of patient in real-time. The result indicates that it will improve the quality and efficiency of the radiotherapy treatment.

Keywords: Binocular Location, Orientation Registration Apparatus, Computed Tomography, Radiotherapy.

1. INTRODUCTION

Requirements for real-time patient positioning accuracy are more demanding when fields are increasingly conformal to the target and the dose-ratio is higher for the realization of the precise radiotherapy. Since the three-dimensional (3-D) noncoplanar fields are employed, the real-time positioning accuracy has been more difficult to achieve practically,[1,2] and the rotation errors are even harder to be obtained.[3,4] With the development of the Image-guided Radiotherapy (IGRT), high-precision positioning techniques which will improve the accuracy and efficiency get lots of interest. Surface alignment technique,[5,6] Ultrasound-guided positioning techniques,[7,8] and Optically-guided technique[9–11] are common guided patient positioning techniques. Currently, the setup errors detection methods are most commonly used depending on the visualization of anatomic landmarks that rely on the portal images.[12,13] As a result, the efficiency is too low to be real-time, and not all the errors of the six freedom degree can be detected.

As the binocular vision[14,15] technology becomes more matured over time, the binocular location is introduced into radiotherapy. Recently, methods for determining patient posture using radio-opaque markers affixed to the patient have been proposed, the 3-D spatial location of these markers can be detected from two projection-images.[16,17] However, these methods also rely on the portal images that can reduce the efficiency. Nevertheless, the markers should be detected in real-time, and the 3-D spatial translation and rotation can be quantified. As the markers can be detected rapidly, they should be easily tracked actively or passively. We chose the passive method where we used high refractive index glass beads markers instead of the radio-opaque markers. The high refractive index glass beads have the characteristic that visible light will be reflected back in the parallel direction to the incident angle[18,19] so that the markers can be detected easily in the binocular images.

*Author to whom correspondence should be addressed.

To be real-time, markers detection and quantization of the 3-D spatial translation and rotation should be automated. We introduced the Polaris system[20–22] to help us implement the markers detected, and developed a method for the real-time quantization of the 3-D spatial errors of the six degrees of freedom. This method is based on the localization of the markers affixed to the surface of a phantom temporarily.

Currently, Simulation Localization System including X-Ray Simulation, CT-Simulation, etc. and Image-Guide Radiation Therapy (IGRT) including Electronic Portal Imaging Device (EPID), Cone Beam Computed Tomography (CBCT), etc. are the most commonly used system which are called Common Positioning System (CPS) here.

In CPS, which cannot provide the real-time tracking, the accuracy of non-coplanar positioning depends on the treatment couch accuracy, laser light, portal images of simulation and so on. The Optical Positioning System (OPS) can monitor the three-dimensional (3-D) spatial position of patient in real time by tracking passive markers affixed to the surface of patient whose accuracy depends on the NDI markers tracking system.

In Section 2, positioning principle and non-coplanar positioning method of OPS are briefly introduced, meanwhile, the comparison experiment is also introduced. The results are reported and discussed in Sections 3 and 4 respectively.

2. METHODS AND MATERIALS

2.1. Positioning Method

There are four key steps to implement real-time monitoring in the clinical environment. Firstly, we registered the isocenter of accelerator and the coordinate axes vectors of the treatment couch using the Orientation Registration Apparatus (ORA). Secondly, we prepared the phantom by affixed number of markers to the phantom surface, and made sure that the couch in Computed Tomography (CT) room horizontal, and then took the CT scanning. Thirdly, we designed the treatment plan from which we obtained the coordinates of the markers and treatment center in CT coordinate system. Finally, we began the real-time monitoring, during this process, we matched the markers in the data from CT and the data from Polaris system, and performed some matrix operations. These operations are introduced in detail using Figure 1.

2.2. Orientation Registration Apparatus

We developed an apparatus to register the coordinate system of the treatment couch for quantization of the 3-D spatial errors of the six degrees of freedom, we called it the Orientation Registration Apparatus (ORA). As shown in Figure 2, there are three markers in ORA, which are labelled as A, B, C respectively, and these will be detected by the Polaris system. We defined the line passing through A and B as the X axis, $\overrightarrow{AB} \times \overrightarrow{AC}$ is defined as Y axis, and Z axis is X axis cross product Y axis. Prior to positioning, we placed the ORA on the platform, and we adjusted it to be horizontal, with the intersection of the two graduation lines aligned to the isocenter of the accelerator, and the graduation line, which pass through A and B aligned to one of the light field cross lines that are parallel to X axis of the treatment couch. Then, our system records the isocenter location and the vectors of treatment couch coordinate axes in the Polaris coordinate system.

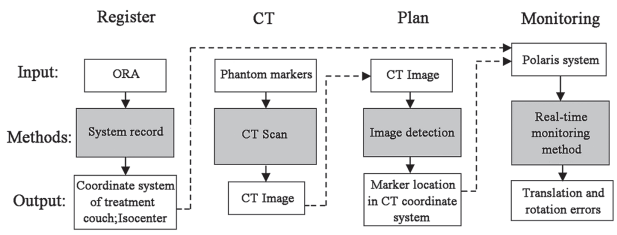

Fig. 1. Flow chart depicting operation of the monitoring me. There are four steps (registration of isocenter, CT scanning, planning and monitoring) of which the first three are the preparation for monitoring. And most computation is conducted during the fourth step.

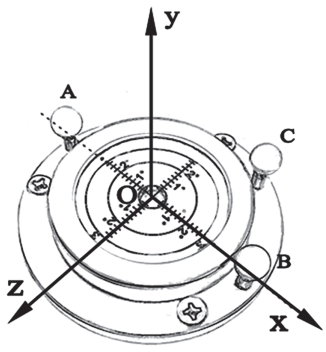

Fig. 2. Orientation registration apparatus. There are three markers fixed in it, and two orthogonal graduation line on it; Of the two lines, one line passes through the markers *A* and *B*, and the direction is established by cross of *AB* and *AC*.

2.3. Quantization of the 3-D Spatial Translation and Rotation

There are three coordinate systems (CS), namely, the (1) CT CS, (2) Polaris CS and (3) ORA CS, respectively. The transformation between the CT CS and Polaris CS are shown in Eq. (1) below:

$$\begin{bmatrix} x_{\mathrm{Po}} \\ y_{\mathrm{Po}} \\ z_{\mathrm{Po}} \\ l \end{bmatrix} = P_{\mathrm{cp}} \cdot \begin{bmatrix} x_{\mathrm{CT}} \\ y_{\mathrm{CT}} \\ z_{\mathrm{CT}} \\ l \end{bmatrix} \tag{1}$$

$$P_{\mathrm{cp}} = \begin{bmatrix} \cos\varphi_{\mathrm{cp}}\cos\theta_{\mathrm{cp}} & \sin\varphi_{\mathrm{cp}}\cos\theta_{\mathrm{cp}} & -\sin\theta_{\mathrm{cp}} & T_x \\ \cos\varphi_{\mathrm{cp}}\sin\theta_{\mathrm{cp}}\sin\gamma_{\mathrm{cp}} - \sin\varphi_{\mathrm{cp}}\cos\gamma_{\mathrm{cp}} & \sin\varphi_{\mathrm{cp}}\sin\theta_{\mathrm{cp}}\sin\gamma_{\mathrm{cp}} + \cos\varphi_{\mathrm{cp}}\cos\gamma_{\mathrm{cp}} & \cos\theta_{\mathrm{cp}}\sin\gamma_{\mathrm{cp}} & T_y \\ \cos\varphi_{\mathrm{cp}}\sin\theta_{\mathrm{cp}}\cos\gamma_{\mathrm{cp}} + \sin\varphi_{\mathrm{cp}}\sin\gamma_{\mathrm{cp}} & \sin\varphi_{\mathrm{cp}}\sin\theta_{\mathrm{cp}}\cos\gamma_{\mathrm{cp}} - \cos\varphi_{\mathrm{cp}}\sin\gamma_{\mathrm{cp}} & \cos\theta_{\mathrm{cp}}\cos\gamma_{\mathrm{cp}} & T_z \\ 0 & 0 & 0 & 1 \end{bmatrix} \tag{2}$$

where x_{CT}, y_{CT} and z_{CT} are the 3-D coordinates of any point in the CT coordinate system while x_{Po}, y_{Po} and z_{Po} represent the 3-D coordinates of any point in the Polaris coordinate system. The transformation is based on P_{CP} that is a 4×4 matrix. Then,

γ_{CP}, and φ_{CP}, θ_{CP} are the rotation angles[23,24] of the roll, pitch, and yaw respectively. T_x, T_y and T_z are the translations in LR, IS and AP directions respectively.[25–27]

The transformations between ORA CS and Polaris CS as shown in Eq. (3) as below:

$$\begin{bmatrix} x_{Po} \\ y_{Po} \\ z_{Po} \\ l \end{bmatrix} = P_{op} \cdot \begin{bmatrix} x_{ORA} \\ y_{ORA} \\ z_{ORA} \\ l \end{bmatrix} \tag{3}$$

$$P_{op} = \begin{bmatrix} \cos\varphi_{op}\cos\theta_{op} & & & \\ \cos\varphi_{op}\sin\theta_{op}\sin\gamma_{op} - \sin\varphi_{op}\cos\gamma_{op} & & & \\ \cos\varphi_{op}\sin\theta_{op}\cos\gamma_{op} + \sin\varphi_{op}\sin\gamma_{op} & & & \\ 0 & & & \end{bmatrix}$$

$$\begin{bmatrix} \sin\varphi_{op}\cos\theta_{op} & -\sin\theta_{op} & T_x \\ \sin\varphi_{op}\sin\theta_{op}\sin\gamma_{op} + \cos\varphi_{op}\cos\gamma_{op} & \cos\theta_{op}\sin\gamma_{op} & T_y \\ \sin\varphi_{op}\sin\theta_{op}\cos\gamma_{op} - \cos\varphi_{op}\sin\gamma_{op} & \cos\theta_{op}\cos\gamma_{op} & T_z \\ 0 & 0 & 1 \end{bmatrix} \tag{4}$$

where X_{ORA}, Y_{ORA} and z_{ORA} represent the 3-D coordinates of any point in the ORA coordinate system. The 4×4 transformation matrix P_{op}, γ_{op}, φ_{op} and θ_{op} are the rotation angles of roll, pitch, and yaw respectively.

After taking in account the treatment center coordinates in Eq. (1), we can obtained the real-time treatment center in Polaris CS, and the deviation to the isocenter and the translations in LR, IS, and AP directions consequently. If the phantom do not have any rotation, the platform on CT couch and platform on treatment couch are all horizontal and the definition of the ORA coordinate system is parallel to the CT coordinate system, the differences between $[\gamma_{op}, \varphi_{op}, \theta_{op}]$ and $[\gamma_{cp}, \varphi_{cp}, \theta_{cp}]$ are 0. But if rotation occurs, the differences represent the rotation angles of roll, pitch, and yaw respectively.[27]

So, the quantization of the 3-D spatial translation and rotation depends on the real-time computation of the transformation matrix because of the markers in CT images and since the real-time monitoring view are corresponding, so we can use the least square[28–30] method to compute the transformation matrix. In order to get the 4×4 matrix,[26] there should be at least 3 markers, and then the fourth 3-D spatial point can be generated by cross product. Next, the influence of the markers number on the accuracy of our proposed method will be discussed subsequently.

2.4. Dose Distribution Calculation

We chose the pencil beam model to calculate the dose distribution which was separated into a central-axis term and an off-axis term, the dose of one point could be expressed in discrete form as:

$$D(X, Y, Z; A) = \sum\sum B(x', y', z) F(x - x', y - y') \tag{5}$$

where x, y and z are the coordinates of the point, A is the area of target, z is the depth of the point to be calculated to the source point, $B(x', y', z)$ is the contribution of the pencil beam to the point to be calculated. The pencil beam distribution was measured in advance which is different from the Gaussian model.

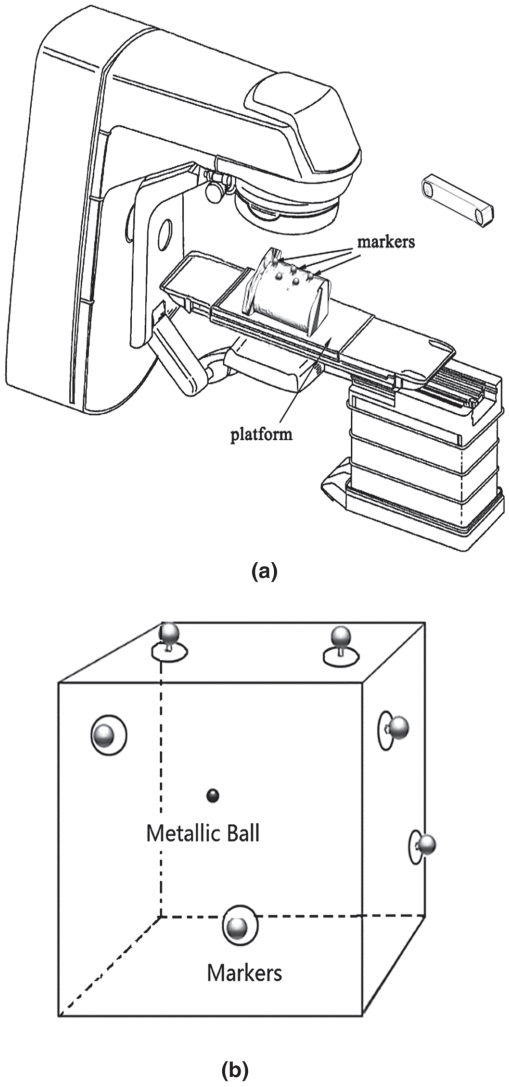

Fig. 3. The monitoring instrumentation and the phantom. (a) A number of markers are affixed to the phantom, and there is a platform under the phantom for the movement of the roll and the title, the platform was placed on the treatment couch which can be translated and rotated; (b) The phantom. The metallic ball which was placed inside the phantom is considered as the treatment center, and there were several markers affixed to the phantom for tracking.

$F(x - x', y - y')$ is the proportion between the axis-center point and the point to be calculated in the same layer in which the point to be calculated lays, and it was a monotone increasing function which meant that as $x - x'$ and $y - y'$ increase, the value of $F(x - x', y - y')$ will also increase.

The dose will change of certain percentage caused by the deviation of the positioning is expressed as:

$$\Delta D(x, y, z; A) = \sum\sum B(x', y', z)(F(x - x'', y - y'') - F(x - x', y - y')) \tag{6}$$

where $(x - x'', y - y'')$ depicts the different off-axis ratio that is caused by the deviation of the positioning, so the smaller deviation is, the smaller the dose changes.

2.5. Experimental Method

In our study, we compared the accuracy of CBCT system, CT-Simulation system and the OPS in absolution location. Prior to the experiment, a 1 mm diameter metallic ball was placed inside the phantom to representative the isocenter, and a certain number of high refractive index glass beads markers were affixed to the phantom surface in different shape and with different relative position of isocenter as shown in Figure 3(b).

The phantom was affixed to a platform that can be rolled and tilted, and the platform was placed on the treatment couch of the Varian accelerator, which can translated and rotated. As a result, the six degrees of freedom of the phantom can be modified and measured. The resolution of the translation readouts for couch motion was 1 mm, and the resolution of the yaw angle is 0.1°. The roll and pitch of the platform can be measured by the Electronic Digital Inclinometer (EDI), which has the resolution of 0.1°.

We conducted 50 experiments under different conditioning in order to verify the accuracy of this method. Here, we divided these 50 experiments into five sets. In each set, the number of markers affixed to phantom is the same, but the relative position between markers and treatment center are different. For the verification of absolution location in each experiment, we opened the phantom after finishing the set-up to measure the errors in LR and AP directions directly and record the current couch height ($h1$). Subsequently, we adjusted the Source-Surface-Distance (SSD) to 1000 mm and recorded the current couch height ($h2$). Then, we get the error in IS direction as $h1 - h2$. To verify the relative movement and for the further analysis, the move range of the couch in every direction was set between 0 mm–20 mm, and the rotation range was set between 0° to 45°. We recorded each of the readouts and the measured data, then we get the errors by subtracting the measured data from the readouts.

3. RESULTS AND DISCUSSION

3.1. Accuracy of Absolution Location

As shown in Figure 4(a), the mean translation setup errors of both OPS and CBCT are all around 0.5 mm in three directions. By contrast, CT-Simulation whose mean translation errors are all over 1.5 mm and even up to 2.0 mm in IS direction had a poor performance in translation accuracy. Figure 4(b) shows us that both CBCT and CT-simulation have the rotation errors around 2.0° in pitch, yaw and roll directions. For OPS, the mean rotation errors are all below 0.5°.

Even the translation accuracy of CBCT is up to the clinic requirement, but we find that during the process of setup, rotation errors in three directions are out of consideration that even the treatment center is setup correctly, the wrong patient posture will reduce the treatment effect. In the experiment, we found that the procedure of CBCT setup take too long time which range from 5 minutes to 10 minutes. It will increase the patients' discomfort, and it shows that CBCT cannot provide the real-time monitoring. For CT-Simulation, both the translation and the rotation errors are all bigger than those of CBCT and OPS, and the process also takes too long time. By contrast, OPS had a good performance in either translation accuracy or rotation accuracy. Besides, the procedure of OPS setup only take about 30 seconds which will contains a few operation.

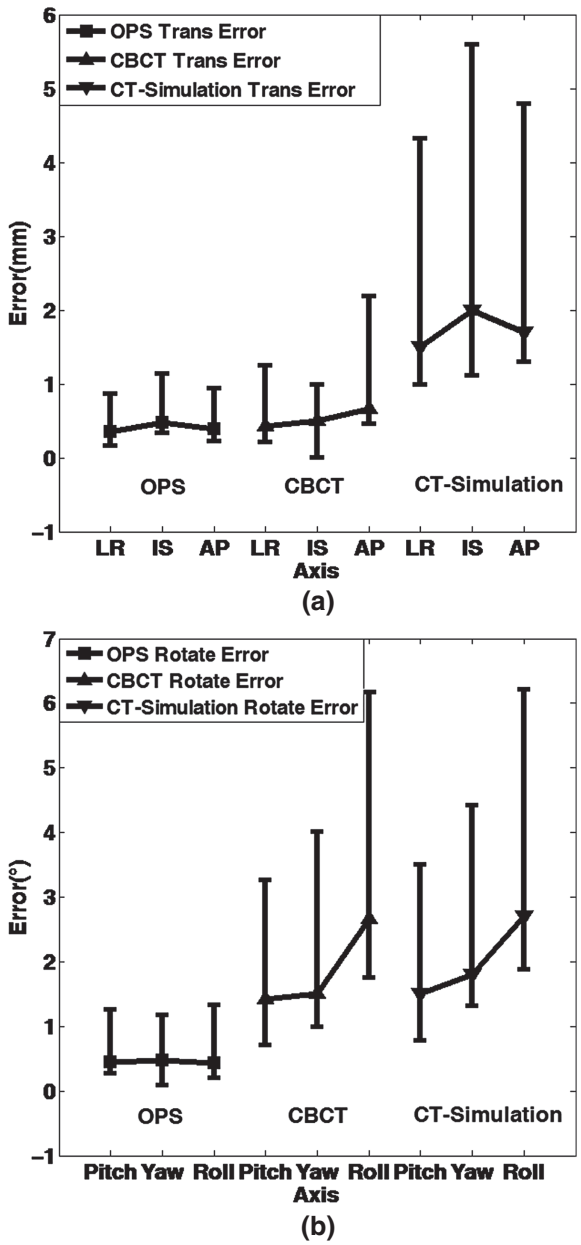

Fig. 4. Accuracy of the methods in translation and rotation of absolute location. Herein, (a) comparison of translation errors among OPS, CBCT and CT-simulation in left to right (LR), inferior to superior (IS), and anterior to posterior (AP) directions respectively; (b) comparison of rotation errors among OPS, CBCT and CT-simulation in the roll, pitch and yaw directions respectively.

3.2. Accuracy of Relative Movement

After the initial setup is implemented, the phantom was moved either by translation or by rotation to a new posture. At the meantime, the couch or EDI readouts and the real-time readouts of monitoring system were recorded, which we defined them as prescribed data and computed data respectively. Between the prescribed and computed data, the maximum difference for translation is 0.94 mm, and for rotation is 1.24°. The standard deviation (SD) is 0.23 mm for LR, 0.16 mm for IS, and 0.16 mm for AP. The SD are 0.28°, 0.18°, and 0.27° for roll, pitch and yaw respectively. As demonstrated in Figure 5, a larger error is accompanied

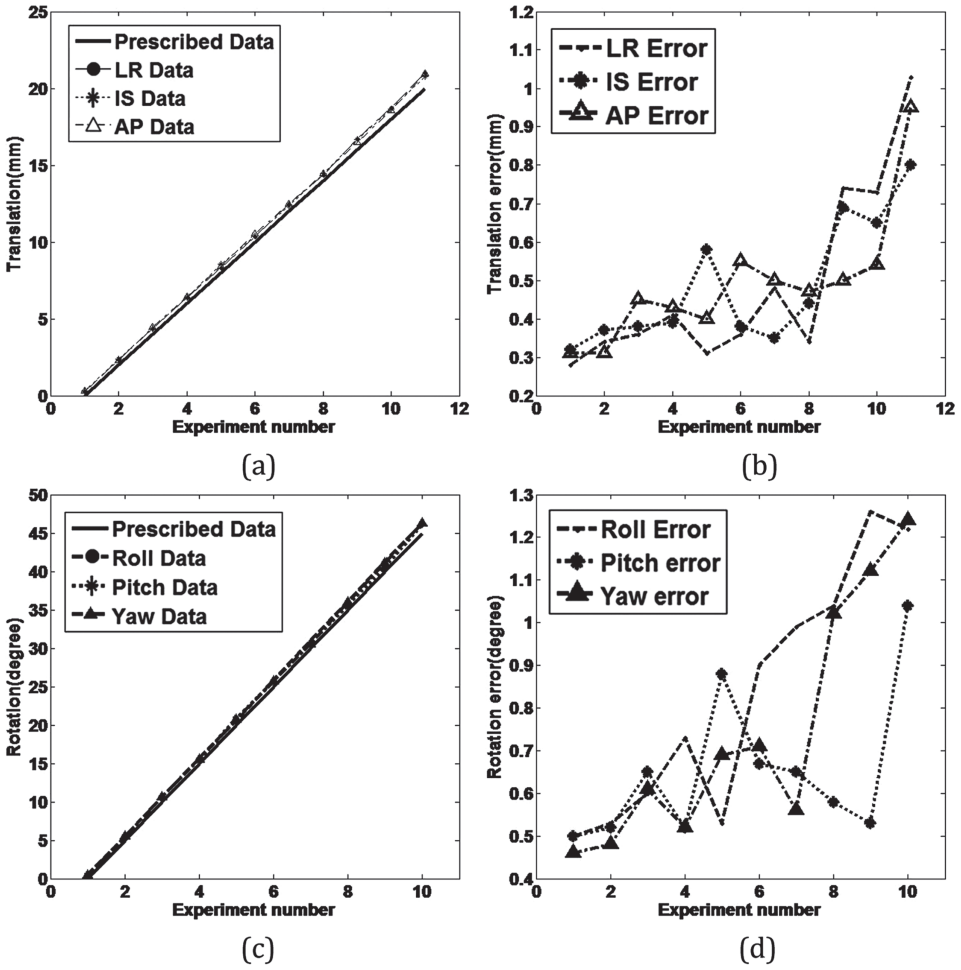

Fig. 5. Accuracy of the method in translation and rotation of relative location. Herein, (a) comparison of the prescribed data and measured data in translation; (b) location errors in translation; (c) comparison of the prescribed data and measured data in rotation; and (d) location errors in rotation.

by more translation or rotation of the phantom. This is because if the translation or rotation is large enough that some of the markers are out of the monitoring scope, then the precision will decrease.

3.3. Influence of Markers Number to Accuracy

We divided the 50 experiments into 5 sets by the number of markers (ranging from 3 to 7) affixed to the phantom. As from Table 1, the translation and rotation errors of the measured data are presented, and when the markers number is less than 6, the number of markers corresponds to the accuracy of the computed data. When the markers number is more than 6, the accuracy tends to be stable; and then for rotation, the markers number should be kept at 5 to maintain stability. Therefore, in order to have high accuracy, the markers number should not be less than 6.

Table I. Translation and rotation errors of measured data.

	Translation error (mm)			Rotation error (°)		
Number of markers	LR	IS	AP	Roll	Pitch	Yaw
3	0.36	0.36	0.34	0.55	0.55	0.56
4	0.29	0.29	0.34	0.53	0.5	0.52
5	0.28	0.28	0.32	0.51	0.5	0.47
6	0.28	0.28	0.28	0.47	0.5	0.48
7	0.27	0.27	0.32	0.5	0.5	048

4. CONCLUSIONS

This paper focus on the comparison between CPS and OPS non-coplanar positioning for treatments of nasopharyngeal carcinoma. The result shows that CPS positioning has a mean deviation of 2.60 mm, which will increase the dose received by OARs or even make the dose over the tolerated dose. In contrast, the mean deviation of OPS positioning method we proposed is 0.36 mm which will have more effect on the dose distribution. In the case that the beams are near the OARs, the advantage of OPS positioning is particularly significant.

Acknowledgment: This work is supported by the National Nature Science Foundation of China (81371638, 11272329), Fundamental Research Funds for the Central Universities (1106021034), Jiangsu Provincial Nature Science Foundation of China (BE2012158, BK2011393 and BY2012186), National Natural Science Foundation of China (Grant No. 11475087).

References and Notes

1. D. F. DeMenthon, Computer vision system for position monitoring in three dimensions using non-coplanar light sources attached to a monitored object: U.S. Patent 5,227,985, 1993-7-13.
2. J. A. Speasl and L. Schupak, Positioning system and method: U.S. Patent 5,815,114, 1998-9-29.
3. U. A. van der Heide, A. N. Kotte, H. Dehnad, P. Hofman, J. J. Lagenijk, and M. van Vulpen, Analysis of fiducial marker-based position verification in the external beam radiotherapy of patients with prostate cancer. *Radiotherapy and Oncology* 82, 38 **(2007)**.
4. M. J. Murphy, Fiducial-based targeting accuracy for external-beam radiotherapy. *Medical Physics* 29, 334 **(2002)**.
5. S. W. Hadley, L. S. Johnson, and C. A. Pelizzari, Video based surface alignment technique for 3D patient positioning, *Engineering in Medicine and Biology Society, 2000. Proceedings of the 22nd Annual International Conference of the IEEE, IEEE, 2000*, Chicago, Illinois, USA, July **(2000)**, Vol. 4, pp. 2735–2736.
6. S. Ju, C. Hong, J. Kim, E. Shin, Y. Han, Y. Ahn, D. Choi, H. Park, and W. Huh, Development of a video-guided real-time patient motion monitoring systema. *Medical Physics* 39, 2396 **(2012)**.
7. S. L. Meeks, J. M. Buatti, L. G. Bouchet, F. J. Bova, T. C. Ryken, E. C. Pennington, K. M. Anderson, and W. A. Friedman, Ultrasound-guided extracranial radiosurgery: Technique and application. *International Journal of Radiation Oncology® Biology® Physics* 55, 1092 **(2003)**.
8. L. G. Bouchet, S. L. Meeks, F. J. Bova, J. M. Buatti, and W. A. Friedman, Three-dimensional ultrasound image guidance for high-precision extracranial radiosurgery and radiotherapy, Radiosurgery, Karger Publishers **(2002)**, Vol. 4, pp. 262–278.
9. H. Yan, F.-F. Yin, and J. H. Kim, A phantom study on the positioning accuracy of the Novalis Body system. *Medical Physics* 30, 3052 **(2003)**.
10. S. Klöck and R. G. Müller, An exact and objective positioning system for patients in conformal radiotherapy basing on optical 3D-surface-detection, *Engineering in Medicine and Biology Society, 2000. Proceedings of the 22nd Annual International Conference of the IEEE. IEEE, 2000*, Chicago, Illinois, USA, July **(2000)**, Vol. 3, pp. 2184–2185.
11. H. P. Kim, Y. K. Kim, II, H. Lee, and S. J. Ye, Development of an optical-based image guidance system: Technique detecting external markers behind a full facemask. *Medical Physics* 38, 3006 **(2011)**.
12. B. E. Cochran, The Effect of Treatment Couches on Delivered Dose During Radiotherapy Treatments, Master's Thesis, San Diego State University **(2012)**.
13. T. Willoughby, J. Lehmann, J. A. Bencomo, S. K. Jani, L. Santanam, A. Sethi, T. D. Solberg, W. A. Tomé, and T. J. Waldron, Quality assurance for nonradiographic radiotherapy localization and positioning systems: Report of task group 147. *Medical Physics* 39, 1728 **(2012)**.
14. H.-Y. Li and X.-S. Zhang, Binocular location model of digital camera based on geometric invariant under projective transformation. *Journal of Shanghai University of Engineering Science* 4, 013 **(2009)**.
15. Z. Zi-Xiaoa, Z. Xiao-linb, H. U. Fengb, and Z. Lib, Binocular stereo location on emulator robot. *Video Engineering* 8, 034 **(2010)**.
16. M. D. Altschuler, P. Findlay, and R. D. Epperson, Rapid, accurate, three-dimensional location of multiple seeds in implant radiotherapy treatment planning. *Physics in Medicine and Biology* 28, 1305 **(1983)**.
17. J. L. Robar, A. Day, J. Clancey, R. Kelly, M. Yewondwossen, H. Hollenhorst, Murali Rajaraman, and D. Wilke, Spatial and dosimetric variability of organs at risk in head-and-neck intensity-modulated radiotherapy. *International Journal of Radiation Oncology® Biology® Physics* 68, 1121 **(2007)**.
18. J. Lee and A. Yee, Fracture of glass bead/epoxy composites: On micro-mechanical deformations. *Polymer* 41, 8363 **(2000)**.
19. J. Parr, D. Parkinson, and A. Norman, A glass micro-bead system for the investigation of soil micro-organisms. *Nature* 200, 1227 **(1963)**.
20. R. Khadem, C. C. Yeh, M. Sadeghi-Tehrani, M. R. Bax, J. A. Johnson, J. N. Welch, E. P. Wilkinson, and R. Shahidi, Comparative tracking error analysis of five different optical tracking systems. *Computer Aided Surgery* 5, 98 **(2000)**.
21. A. D. Wiles, D. G. Thompson, and D. D. Frantz, Accuracy assessment and interpretation for optical tracking systems. *Proceedings of SPIE* 5367, 421 **(2004)**.
22. K. Pentenrieder, P. Meier, and G. Klinker, Analysis of tracking accuracy for single-camera square-marker-based tracking, *Proc. Dritter Workshop Virtuelle und Erweiterte Realitt der GIFachgruppe VR/AR, Koblenz, Germany*, Citeseer **(2006)**.
23. Z. Zhang, A flexible new technique for camera calibration. *IEEE Transactions on Pattern Analysis and Machine Intelligence* 22, 1330 **(2000)**.
24. G. K. Cole, B. M. Nigg, J. L. Ronsky, and M. R. Yeadon, Application of the joint coordinate system to three-dimensional joint attitude and movement representation: A standardization proposal. *Journal of Biomechanical Engineering* 115, 344 **(1993)**.
25. S. W. Shepperd, Quaternion from rotation matrix, *Four-Parameter Representation of Coordinate Transformation Matrix* **(1978)**.
26. T. M. Strat, Recovering the camera parameters from a transformation matrix. *Readings in Computer Vision* 93 **(1987)**.
27. W. J. Lloyd, J. D. Meyer, and K. W. W. Yeung, Method and apparatus for calibrated digital printing using a four by four transformation matrix: U.S. Patent 5,508,826, 1996-4-16.
28. K. S. Chua, Efficient computations for large least square support vector machine classifiers. *Pattern Recognition Letters* 24, 75 **(2003)**.
29. J. Steinier, Y. Termonia, and J. Deltour, Smoothing and differentiation of data by simplified least square procedure. *Analytical Chemistry* 44, 1906 **(1972)**.
30. A. Fitzgibbon, M. Pilu, and R. B. Fisher, Direct least square fitting of ellipses. *IEEE Transactions on Pattern Analysis and Machine Intelligence* 21, 476 **(1999)**.

Received: 15 October 2016. Accepted: 12 December 2016.